RSC Advances

ROYAL SOCIETY OF CHEMISTRY

www.rsc.org/advances

RSC Advances

RESEARCH ARTICLE

Manuscript ID : RA-ART-09-2015-017729

Chitosan-graft-PAMAM / alginate core-shell nanoparticles: A safe and promising oral insulin carrier in Animal Model

Received 00th January 20xx,
Accepted 00th January 20xx

DOI: 10.1039/x0xx00000x

www.rsc.org/

P. Mukhopadhyay,[a] and P. P.Kundu[a*]

Efficient, biodegradable and bio-safe polymeric nano carrier in oral insulin delivery is a major thrust in biomedical field. PAMAM grafted chitosan (CS-g-PAMAM) is prepared using a Michael type addition reaction by *grafting* polyamidoanime (PAMAM) onto native chitosan, to improve the water solubility, pH responsiveness, and insulin encapsulation efficiency for the enhancement of relative oral bioavailability of insulin. The insulin loaded nanoparticles were prepared by formation of an ionotropic pre-gelation of an alginate (ALG) core entrapping insulin, followed by PAMAM grafted chitosan (CS-g-PAMAM) polyelectrolyte complexation, to meet successful research in oral insulin. Mild preparation process without involving harsh chemicals is aimed to improve insulin bio-efficiency *in vivo*. The nanoparticles showed excellent core-shell architecture with an average particle size of 98-150 nm in dynamic light scattering (DLS), showing ~97% of insulin encapsulation and 27% of insulin loading capacity. Again, *In vitro* release data confirms a pH sensitive and self sustained release of encapsulated insulin, protecting it from the enzymatic deactivation in the gastrointestinal tract. The oral administration of these nanoparticles exhibits a pronounced hypoglycemic effect in diabetic mice, producing a relative bioavailability of ~11.78%. As no acute systemic toxicity is observed with its peroral treatment, these core-shell nanoparticles can effectively serve as an efficient carrier of oral insulin in mice model.

1. Introduction

Over the last few decades, polymers have been applied to solve the problem of oral insulin delivery using advanced nanotechnology to combat diabetes worldwide. Improvement of poor patient compliance in parenteral insulin delivery is highly possible by choosing the oral route as an alternative.[1] However, several hindrances such as harsh acidic stomach, extensive enzymatic degradation by different proteolytic enzyme of the gastrointestinal tract (GI tract), mucosal surface and tight junction in between the intestinal epithelial cells following oral insulin delivery has to be resolved to achieve ultimate success. In spite of an extensive research, still an efficient oral insulin carrier is not available to meet all theses pressing demands. Nanoparticles of both from natural and synthetic polymers,[2-6] lipids and polysaccharides have gained special attention as efficient drug delivery device for controlled and targeted release, aiming to improve the therapeutic effects by reducing the side effects of the drug formulations. Among them, chitosan (CS) and alginate (ALG) are extensively studied due to their biodegradable, biocompatible, non-toxic and non-immunogenic properties.[7] The CS, a natural polymer with (1-4)-linked 2-amino-2-deoxy-β-D-glucopyranose units, derived from partial deacetylation of chitin (found in crabs, shrimps and lobster shell and in some fungi or yeast) has received considerable attention in oral insulin research for past few decades.[8] It could offer certain advantages over other natural polymers in formulating nanoparticles in a better way for improved oral insulin delivery.[9] Being cationic in nature (pKa 6.5), CS gets easily soluble in aqueous acidic medium by protonation of the amine groups, facilitating effective encapsulation of several bio-molecules (proteins, drugs, DNA) etc by electrostatic interaction. Furthermore, multiple functional groups ($-NH_2$ and $-OH$) on its structure could prolong the resident time in the GI tract and aids sustained release of encapsulated insulin.[10] Apart from the endowment of positive charge on the surfaces of nanoparticles, CS also elevates the interaction time with intestinal epithelium enhancing permeation through tight junction of intestinal epithelium via paracellular transport.[11] Most importantly, it is digested by chitosanase enzymes

[a] *Address here.*
[b] *Address here.*
[c] *Address here.*
† Footnotes relating to the title and/or authors should appear here.
Electronic Supplementary Information (ESI) available: [details of any supplementary information available should be included here]. See DOI: 10.1039/x0xx00000x

secreted by microorganisms of the intestinal lumen following oral ingestion.[8,12,13] However, acidic chitosan solutions (pH <6.5) may not be desirable in myriad applications in biomedicines.[9] Hence, successive modifications are implemented in order to improve its water solubility, physicochemical and biochemical properties.[14-18] Among them, graft co-polymerization with synthetic polymers has been extensively investigated to get novel biomaterials for successful oral insulin applications.[19] Dendrimers, a new class of synthetic polymers, come into focus possessing highly branched, nano-spherical well defined architectures with precise molecular weight and multivalent functional sites, necessary for oral drug delivery.[20,21] The cationic poly(amidoamine) (PAMAM) dendrimers show high density of primary amino groups at the surface with uniform size, excellent solubility in aqueous medium and non-immunogenic nature, aiding the enhanced delivery of diverse nucleic acids. But, documentation of certain toxicity in higher generation (high density of primary amine groups) may hinder its wide application in insulin delivery.[22] Hence, the chemical combination of chitosan with PAMAM could provide a unique biomaterial with improved water solubility, higher charge density and lower toxicity for effective oral insulin administration.

Alginate (ALG) is another water soluble, pH sensitive natural polysaccharide, containing varying amounts of 1,4-linked β-D-mannuronic acid (M) and α-L-guluronic acid (G) residues, usually extracted from brown seaweed. It has also gained excellent popularity in oral insulin delivery due to its shrinkage in lower pH,[23] enabling complete retention of encapsulated insulin during the passage through the GI tract; hence provide protection against enzymatic deactivation. Again biodegradability, biocompatibility, low toxicity, low immunogenicity and good mucoadhesion[24,25] facilitate its wide application in oral drug delivery research. Nanoparticles can easily be formulated using ALG either by physical or chemical crosslinking for the sustained drug release studies. Again, physical crosslinking is usually preferred over chemical crosslinking[26] to avoid toxicity episodes. Calcium, a divalent cation is reported to crosslink alginate and maintains the biological efficacy of insulin also.[7] The nanoparticles of chitosan and alginate are reported to efficiently protect insulin from the harsh acidic environment of the stomach and offer sustained insulin release in the intestinal milieu.[27] Furthermore, pH sensitive, bio-adhesive chitosan-alginate nanoparticles also showed significant hypoglycemic effects in rat model too.[28] In our previous study, we have successfully synthesized chitosan-alginate nanoparticles core-shell nanoparticles which showed prolonged hypoglycemic effects with ~8.11% insulin bioavailability producing no systemic toxicity within the animal system.[7]

Finally, in the present study, we have prepared and characterized a novel oral insulin carrier system of core-shell nanoparticles using PAMAM grafted chitosan and alginate with comparatively smaller size compared to the previous reports[7,27,28] in order to improve the oral insulin bioavailability in animal models. The co-polymer is novel in terms of easy and mild synthesis process involving no harsh or toxic chemicals, and it also provides higher charge density with lower toxicity for effective oral insulin administration. Novelty also lies in its structural chemistry; the core-shell architecture of the nanoparticles, prepared by using this unique biopolymer, helps to reduce particle size; it allows easy internalization through the tight junctions between intestinal epithelial cells and ensures effective protection to insulin molecules from harsh gastrointestinal enzymes by sheltering it within the core of the nanoparticles. All the physical characterizations of nanoparticles and their insulin loading capacity, insulin encapsulation efficiency, *in vitro* insulin release, *in vivo* pharmacological responses, and insulin bioavailability are investigated in details in this article. Furthermore, a detailed *in vivo* systemic toxicity study has been carried out following oral delivery of these nanoparticles to have an idea about the safety measures of the novel carrier system.

2. Experimental

2.1. Materials

Chitosan, molecular weight (MW) 222 kDa, degree of deacetylation (DDA) 82% was obtained from Himedia (India). Low molecular weight chitosan (25 kDa, DDA 82%) was prepared by oxidative degradation using sodium nitrite (Merck, India) at room temperature according to our previous method.[8] Low viscosity, low-G (α-L-guluronic acid) ALG (β-D mannuronic acid (M)/α-L-guluronic acid (G) content 64.5%/35.5%) was purchased from Loba Chemie, India. The molecular weight of alginate is 103 KDa. Ethylenediamine (EDA), methyl acrylate (MA), creatinine merckotest kit and methanol were purchased from Merck, India. PAMAM dendrimer (G 2.0) was synthesized and PAMAM grafted chitosan was prepared according to the previous reports.[18,29] White crystalline type Potassium bromide (KBr) was purchased from Merck (India). Insulin (Bovine insulin, 27USP units per mg) and alloxan monohydrate were purchased from Sigma-Aldrich. Bovine insulin ELISA kit from LILAC Medicare Pvt. Ltd, serum glutamate pyruvate transaminase (SGPT) ALAT(GPT)-LS kit and serum glutamate oxaloacetate transaminase (SGOT), AST(GOT)-LS kit from Piramal Health care Limited, Mumbai, India and lactate dehydrogenase LDH (P-L) kit from Crest biosystems, Goa, India, creatinine merckotest kit from Merck Limited, Mumbai, India, and micro protein kit from Crest biosystems, Goa, India were purchased. Multistix reagent strips (Siemens, Baroda, India) were used for urine biochemical parameter analysis. Other chemicals of analytical grade were used as received.

Animals

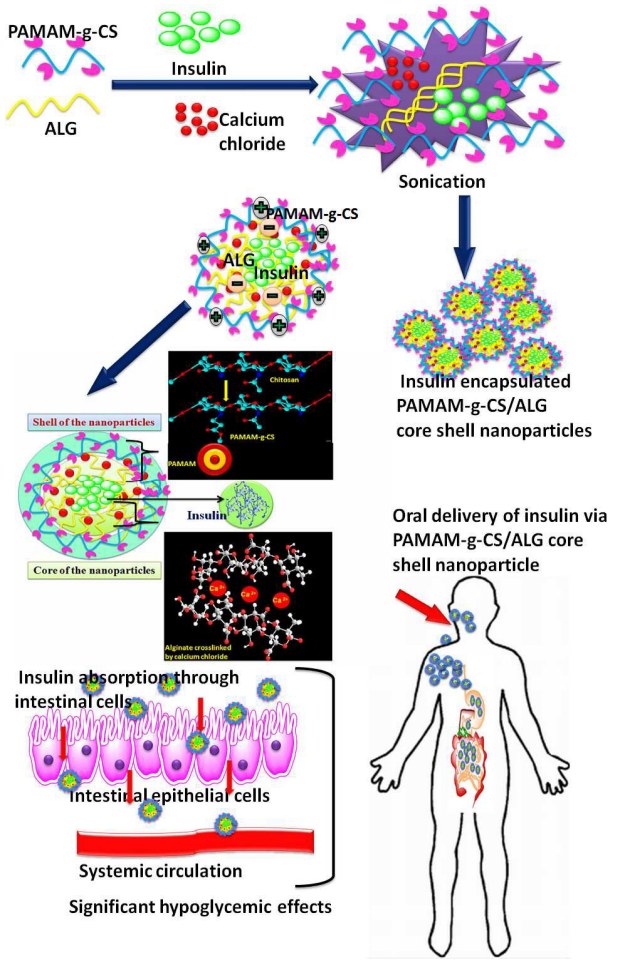

Scheme 1. Schematic diagram showing preparation of insulin-loaded CS-g-PAMAM/ALG core-shell nanoparticles and the chemical structure of the nanoparticles used for successful oral insulin delivery.

Male Swiss albino mice of about 3-4 weeks old, (26±2 g) (from M/s Chakraborty Enterprise, Calcutta, India) were housed under a controlled environment (Room temperature: 23±2 ◦C, relative humidity: 60±5%, 12 hr day/night cycle) with a balanced diet and water *ad libitum*. All the animal experiments were approved by the animal ethical committee, Department of Physiology, Calcutta University, in accordance with the guideline of the committee for the purpose of control and supervision of experiments on animal (CPCSEA Ref no: 820/04/ac/CPCSEA dated 06.08.2004), Government of India.

2.2. Preparation of Chitosan–graft-PAMAM copolymer (CS-g-PAMAM)

CS-g-PAMAM was prepared by two consecutive steps; preparation of N-carboxyethylchitosan methyl ester (NCME) followed by conjugation of PAMAM dendrimer (G 2.0) with N-carboxyethylchitosan methyl ester according to our previous report.[17] N-carboxyethylchitosan methyl ester was prepared according to the previous report with slight modification.[30] At first, chitosan was purified by re-precipitation method prior to the reaction.[8] Then, 1.0 g of purified chitosan was dissolved in 50 mL of 1 % acetic acid solution under constant stirring for 30 min and diluted with 200 mL of ethyl alcohol. To this solution, methyl acrylate (10 equiv/NH2 of chitosan) was added slowly and the reaction was further continued for 48 hr at 25 °C. After that, the reaction mixture was concentrated to approx 100 mL under reduced pressure to remove excess amount of methyl acrylate and solvent. The remaining mixture was dialyzed for 3 days against deionised water and lyophilized for another 3 days to obtain N-carboxyethylchitosan methyl ester.

To conjugate PAMAM dendrimer with NCME, N-carboxyethylchitosan methyl ester (100 mg) was dispersed in methyl alcohol (50 mL) and then, PAMAM (0.54 mmoL: 1.0 equiv/CO2Me) in MeOH (50 mL) was added to this suspension. The reaction mixture was allowed to stir at room temperature. After 3 days, the mixture was evaporated to dryness and dispersed in 0.2 M NaOH solution for 2 hr at room temperature, dialyzed and finally lyophilized to get the final product.

2.3. Preparation of blank chitosan-alginate (CS/ALG) and Chitosan-graft-PAMAM-alginate (CS-g-PAMAM/ALG) core-shell nanoparticles

Blank core-shell nanoparticles were prepared, initially by dissolving ALG in distilled water at a final concentration of 3.0 mg/mL and then the pH of the solution was adjusted to 5.1. Further, calculated amount of CS and CS-g-PAMAM were dissolved in 1 % acetic acid solution and in distilled water respectively, under constant stirring for 30 mins at room temperature to prepare CS and CS-g-PAMAM solutions with varying concentrations ranging from 0.25 mg/mL to 3 mg/mL. The pH of the solution was adjusted to 5.5-5.7 by the addition of 0.1 M sodium hydroxide solution. The core-shell nanoparticles were prepared by using a two step method with slight modification as previously reported by Rajaonarivony et al.[31]

At first, aqueous calcium chloride (1mL of 3.35 mg/mL) was added drop wise to 5mL aqueous solution of ALG (3.0 mg/mL) and then sonicated for 15 mins by using a probe ultra sonicator (Q Sonicasonicator). Then 2 mL of each CS solution and CS-g-PAMAM solution (0.25 mg/mL to 3 mg/mL) were added drop wise respectively, to the resultant calcium ALG pre-gel and again sonicated for 25-30 mins at room temperature. The resultant opalescent suspensions were allowed to form nanoparticles of uniform particle size.

2.4. Preparation of Insulin loaded chitosan-alginate (CS/ALG) and Chitosan-graft-PAMAM-alginate (CS-g-PAMAM/ALG) core-shell nanoparticles

The calculated amount of insulin was dissolved in 0.1M HCl solution with a final concentration of 1 mg/mL and then the pH of solution was adjusted to pH 8.0-8.4 by 0.1 N- tris (hydroxymethyl) aminomethane solution. A constant volume of 300 µL insulin solution was then mixed with the calcium chloride solution. Other processes were the same as used above for the preparation of blank nanoparticle. Scheme 1 presents process of core-shell nanoparticle preparation, chemical structure and its efficacy in oral insulin delivery.

2.5. Determination of molecular weight of the polymers and FT-IR spectroscopic analysis

The molecular weight of chitosan and its derivatives were measured by gel permeation chromatography (GPC). The GPC equipment consisted of ultrahydrogel 1000 (7.8 x 300 mm) column, 515 HPLC pump and 2414 RI detector (Waters, USA). The mobile phase was 0.1 M acetic acid/ 0.1 M sodium acetate buffer. Mobile phase and chitosan solution were filtered through 0.45 µm filter (Millipore). The flow rate was maintained at 0.3 mL/min. The sample concentration was 0.3 mg/mL. Polyethylene glycol (Sigma-Aldrich) standards were used to calibrate the column. All data provided by the GPC system were analyzed using the Empower 2 software package.

Fourier transform infrared (FT-IR) analysis was carried out with ATR-FT-IR (model-Alpha, Bruker, Germany) spectrometer, scanning from 4000 to 500 cm^{-1} for 42 consecutive scans at room temperature. All the samples were separately mixed with KBr and pressed into pellets for measurements.

2.6. Determination of particle size and zeta potential

The particle size and zeta potential of insulin loaded CS/ALG and CS-g-PAMAM/ALG core-shell nanoparticles were determined using Dynamic light scattering (DLS) with Zetasizer Nano ZS (Malvern Instrument, UK).

2.7. Scanning electron microscopy (SEM)

The scanning electron microscopy was also carried out to check the size and the surface morphology of insulin loaded CS/ALG and CS-g-PAMAM/ALG core-shell nanoparticles. About 10-12 µL of sample was dropped on a piece of glass slide and dried at room temperature. Then samples were attached to the stub and sputter coated with a thin layer of gold under vacuum to neutralize the charging effects prior to scan in SEM (Hitachi, Japan, Model: 3400N) with an acceleration voltage of 20kV.

2.8. Insulin loading and insulin encapsulation efficiency of CS/ALG and CS-g-PAMAM/ALG core-shell nanoparticles

Both of insulin loaded CS/ALG and CS-g-PAMAM/ALG core-shell nanoparticle solutions were centrifuged at 14,000 rpm/min for 30 mins at room temperature. The clear supernatant was analyzed for insulin content using a UV-vis spectrophotometer (LAMBDA-25, Perkin Elmer, USA) at 280 nm. All experiments were done in triplicate to calculate insulin loading capacity (LC) and encapsulation efficiency (EE) by the following formula:[17]

$$\mathrm{LC}\,(\%) = \frac{\text{Total amount of insulin - free insulin in the supernatant}}{\text{Weight of the nanoparticles}} \times 100 \quad \text{.....(1)}$$

$$\mathrm{EE}\,(\%) = \frac{\text{Total amount of insulin - free insulin in the supernatant}}{\text{Total amount of insulin}} \times 100 \quad \text{.....(2)}$$

2.9. *In vitro* insulin release profile

To determine the insulin release profiles from insulin loaded CS/ALG and CS-g-PAMAM/ALG core-shell nanoparticles, freeze dried samples (~ 50 mg) were immersed in buffer solutions (~ 75 mL) at different pH corresponding to GI tract (i.e., pH 1.2, pH 6.8 and pH 7.4) with mild agitation at 37 °C temperature. At specific time intervals, the samples were centrifuged and an aliquot from each sample was taken out. The concentration of the released insulin in the aliquot of each sample was determined by using a UV spectrophotometer at 280 nm.[7,17] To deduce the insulin release mechanism, the *in vitro* insulin release data were fitted to Ritger-Peppas model.[32,33]

$$\frac{M_t}{M_\infty} = K t^n \quad \text{.....(3)}$$

where, M_t and M_∞ are the absolute amount of insulin released at time (t) and infinite time, respectively; K is a constant showing structural and geometric characteristic of the device, n is the release exponent reflecting the diffusion mechanism. Values of release exponent (*n*) = 0.45, 0.45 < n < 0.89 and 0.89 indicate, Fickian (Case I) diffusion, non-Fickian (anomalous) transport, and diffusion and zero-order (Case II) transport, respectively.

2.10. *Ex vivo* mucoadhesion studies

Mucoadhesion studies were carried out on the freshly excised tissue of the small intestinal of mice according to a previously described method with a slight modification.[17,34] Male Swiss albino mouse (~ 28 g) was sacrificed by overdose of anesthesia and small intestine was carefully removed from the animal body. Saline was flushed through freshly excised intestinal tissue to remove luminal contents and very carefully cut opened. Then the tissue was placed in a glass support with the help of adhesive. The nanoparticles (freeze dried) were uniformly spread and allowed to interact with the intestinal mucosal lining for 10-15 mins and then were mounted at an angle of 45° on a platform under a constant flow rate (10 mL/min) of phosphate buffer (pH 7.4). The percentage of the nanoparticles adhered on the intestinal lumen was calculated

by comparing the weights of adhered particles and applied particles.

2.11. *In-vivo* pharmacological response of insulin loaded CS/ALG and CS-g-PAMAM/ALG core-shell nanoparticles

Diabetic animal model was prepared by interperitoneal alloxan administration in swiss albino mice.[7,17] The diabetic mice were fasted overnight prior to treatment and remained fasted for another 12 hr during the experiment, only allowed water *ad labitum*. Insulin loaded CS/ALG and CS-g-PAMAM/ALG core-shell nanoparticles (~ 500 µL) with a dose of insulin (50 IU/kg b.w) were orally delivered to the diabetic animals (n=6 each group) using a feeding needle. Mice with subcutaneous injection of 500 µL insulin solution (5.0 IU/kg b.w) were used as control. The blood samples (single drop, ~ 20 µL) of the treated and control animals were taken from tail vein and blood glucose level was checked at regular time interval (2 hr) using Bayer's glucose meter.

2.12. Determination of serum insulin and relative insulin bioavailability after oral administration of insulin loaded CS/ALG and CS-g-PAMAM/ALG core-shell nanoparticles

To determine oral insulin bioavailability, initially, diabetic mice were randomly divided into four groups (n=6) and they were treated with oral insulin. The following formulations were administered to each group individually Group I: oral insulin solution (50 IU kg^{-1} b.w), Group II & III: oral insulin-loaded CS/ALG nanoparticle (50 IU kg^{-1} b.w) and oral insulin-loaded CS-g-PAMAM/ALG core-shell nanoparticles (50 IU kg^{-1} b.w) and finally Group IV: subcutaneous injection of insulin solution (5 IU kg^{-1} b.w). Blood samples were collected from the tail vein and the blood serum was separated by centrifugation at 5000 rpm, for 10 mins at 4°C and stored at -20°C. Serum insulin levels were quantified using enzyme linked immunosorbent assay (ELISA). The areas under the curves (AUC) of the concentration versus time profiles were calculated using the linear trapezoidal method. The relative bioavailability was calculated from the ratio of the respective AUC of the insulin loaded core-shell nanoparticles orally administered and subcutaneous (SC) doses of insulin.[35] The relative bioavailability of insulin following oral administration of CS/ALG and CS-g-PAMAM/ALG core-shell nanoparticles was calculated by using the following formula:

$$\text{Relative bioavailability} = \frac{AUC_{(Oral)} \times DOSE_{(Sc)}}{AUC_{(Sc)} \times DOSE_{(Oral)}} \times 100\% \quad \text{.....(4)}$$

where, AUC is the total area under the curve of plasma insulin concentration versus time.

2.13. Toxicity assay of the CS/ALG and CS-g-PAMAM/ALG core-shell nanoparticles in animal models

Acute toxicity studies were carried out in Swiss albino mice with the peroral treatment of CS/ALG and CS-g-PAMAM/ALG core-shell nanoparticles at a dose of 300 mg kg^{-1} b.w/day. Experimental animals were divided into the following three groups, each group containing 6 animals - Group I: animals received only 0.5 mL of 0.9% saline perorally, considered as the control, group II: animals received CS/ALG nanoparticles (300 mg kg^{-1} b.w/day) orally and group III: animals received CS-g-PAMAM/ALG nanoparticles (300 mg kg^{-1} b.w/day) orally. On the next day, urine was collected from all groups of animals maintained at the fasting conditions for 24 hr. Then, the animals were anesthetized and ~ 200 µL blood was collected from retro orbital vein and serum was separated.

2.13.1. Liver function test

Blood samples (~ 200 µL) were collected from the mice by retro orbital bleeding into the tubes under anesthesia. Blood serum was separated by centrifugation at 5000 rpm, for 10 min at 4°C and stored at -20°C. Then, the serum was used to estimate the serum glutamate pyruvate transaminase (SGPT) using ALAT(GPT)-LS kit (Piramal Health care Limited, Mumbai, India), serum glutamate oxaloacetate transaminase (SGOT) with AST(GOT)-LS kit (Piramal Health care Limited, Mumbai, India) and lactate dehydrogenase activity (LDH) with LDH (P-L) kit, (Crest biosystems, Goa, India) to analyse the liver function of the mice treated with the core-shell nanoparticles.

2.13.2. Nephro-toxicity test

Urine samples were analyzed for quantitative measurement of creatinine and microprotein to evaluate the nephro-toxicity of CS/ALG and CS-g-PAMAM/ALG nanoparticles. Again, urine samples were qualitatively analyzed for urobilinogen, protein, blood, ketone, bilirubin, glucose, pH and specific gravity using multistix reagent strips.

For pathohistological diagnosis, vital organs were examined. The liver, kidney and intestine were fixed in 10% phosphate buffered formalin, and then the tissues were embedded in paraffin and subsequently sectioned. The tissue sections were stained with hematoxylin and eosin (H&E). Stomach was observed. Weight of each organ was examined after treatment with core-shell nanoparticles.

2.14. Statistical analysis

All the acute toxicity results were expressed as a mean±SE, n = 6. The significance level was determined by one-way ANOVA following Tukey's post hoc test. $p < 0.05$ was considered as significant.

3. Result and discussion

During the core-shell nanoparticle formation the molecular weight of CS, CS-g-PAMAM and the β-D-mannuronic acid (M) and α-L-guluronic acid (G) ratio of ALG play a significant role in controlling the physical properties of the core-shell nanoparticles and also influences the conditions of interaction between the polymers and insulin. The molecular weight and

Table 1 Molecular weight, degree of deacetylation and solubility of chitosan and modified chitosan.

Polymeric Compound	Average molecular weight (M_w) (Kda)	Degree of deacetylation (DD%)	Solubility in H_2O
Chitosan	222	86	I
Depolymerized Chitosan	25	85	I
CS-g-PAMAM	42.27	85	S

I= Insoluble, S=Soluble

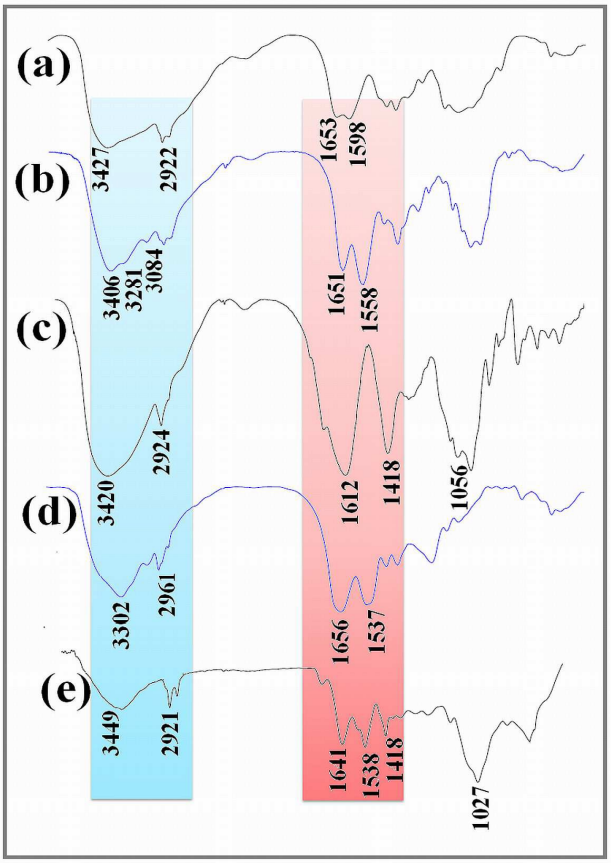

Fig. 1 FT-IR spectra of (a) CS, (b) CS-g-PAMAM, (c) ALG, (d) insulin and (e) core-shell nanoparticles.

the degree of deacetylation (DDA) of CS and depolymerised CS are shown in Table 1. To improve the water solubility of chitosan, CS was depolymerised by oxidation using nitrous acid and the molecular weight of native chitosan was decreased from 222 kDa to 25 kDa. But, its molecular weight was slightly increased from 25 kDa to 42.27 kDa due to the incorporation of PAMAM dendrimer (G 2.0)[17] as shown in Table 1.

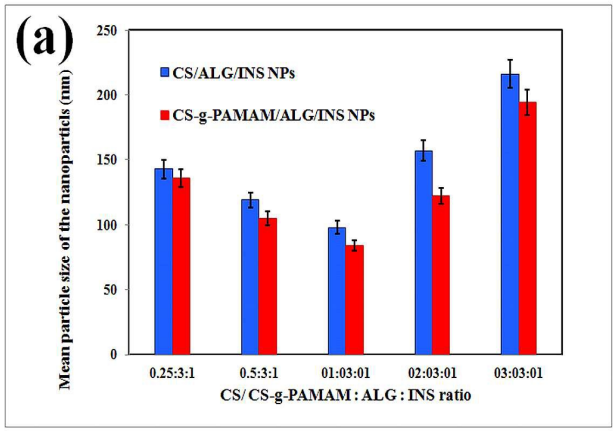

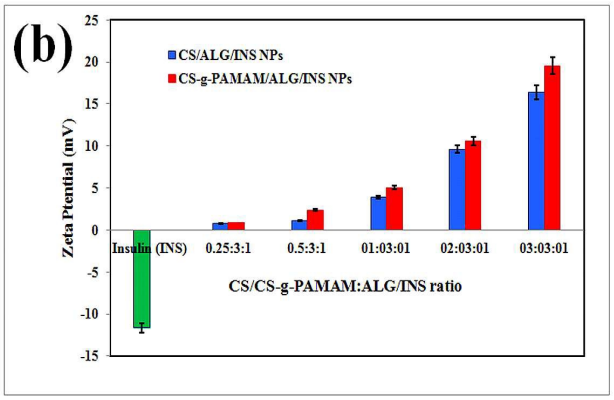

Fig. 2 Comparative analysis of (a) Particle size, (b) zeta potential of insulin loaded CS/ALG and CS-g-PAMAM/ALG core-shell nanoparticles.

3.1. FT-IR spectroscopic analysis

FTIR spectra of polymers and nanoparticle are shown in Fig. 1. The FTIR spectrum of chitosan (Fig. 1a) shows the basic characteristic peaks at 3427 cm^{-1} (O-H stretch and N-H stretch overlap), 2922 cm^{-1} and 2859 cm^{-1} (asymmetric and symmetric stretching of C-H, respectively), 1653 cm^{-1} (NH-CO (I) stretch), 1598 cm^{-1}(N-H bend), 1154 cm^{-1} (bridge –O- stretch), and 1092 cm^{-1} (C-O stretch).[36] Fig. 1b depicts the spectrum of CS-g-PAMAM; it is found that the intensity of absorption peaks at 1651 cm^{-1} (NH CO (I) stretch) and 3282 cm^{-1}, 1558 cm^{-1} (N-H stretching and bending, respectively) is increased after reaction of PAMAM dendrimer (G 2.0) with N-carboxyethylchitosan methyl ester and the peak for ester group at 1728 cm^{-1} is disappeared indicating successful the formation of CS-g-PAMAM from N-carboxyethylchitosan methyl ester. The IR spectrum of ALG (Fig. 1c) shows the basic peaks at 1612 cm^{-1} and 1418 cm^{-1}, assigned to the asymmetric and symmetric stretching of carboxylate salt groups. Additionally, a band around 1056 cm^{-1} (C-O-C stretching) could be attributed to its saccharide structure.[37] Insulin has a characteristic peak at 1656 cm^{-1} (C=O stretching of amide I) and a medium intensity peak at 1537 cm^{-1} of the insulin is

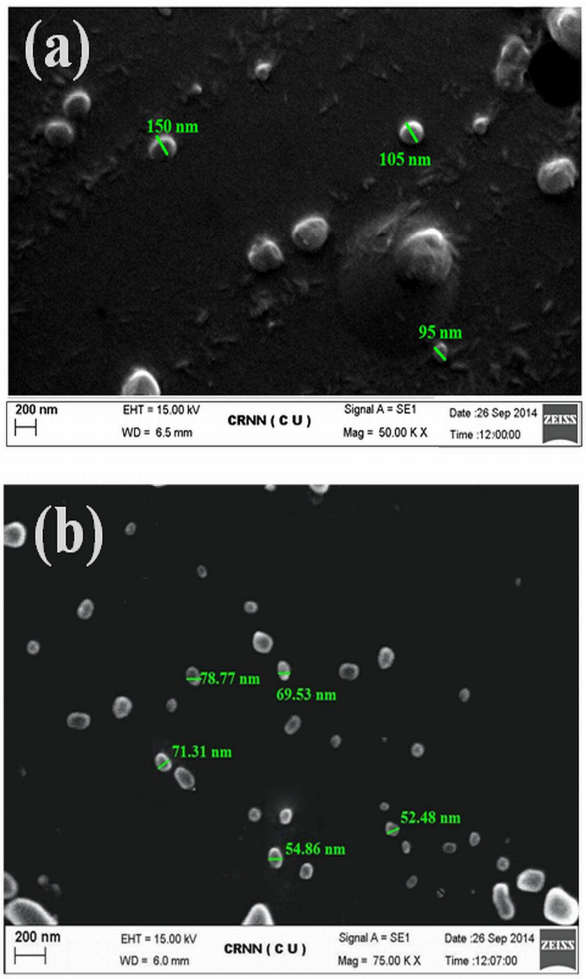

Fig. 3 SEM image of (a) insulin loaded CS/ALG core-shell nanoparticles and (b) insulin loaded CS-g-PAMAM/ALG core-shell nanoparticles.

attributed to the amide-II corresponding to the C–N stretching and N–H bending modes as shown in Fig. 1d. From the IR spectrum of insulin loaded CS-g-PAMAM nanoparticles (Fig. 1e), it is observed that the asymmetrical stretching of $-COO^-$ groups are shifted to 1641 cm^{-1} and the symmetrical stretching of $-COO^-$ groups are shifted to 1418 cm^{-1}. Moreover, the absorption band of CS-g-PAMAM at 1558 cm^{-1} is also shifted to 1538 cm^{-1} after mixing with ALG. The stretching vibration of -OH and $-NH_2$ at 3406 cm^{-1} shifts to 3449 cm^{-1}. So, the FT-IR study suggests that the insulin is encapsulated in the polymeric network and amine groups of CS-g-PAMAM are interacted with the carboxylic groups of ALG to form the core-shell nanoparticles.

3.2. Particle size and zeta potential analysis

An appropriate particle size of nanocomplexes is a very essential parameter for improved oral insulin delivery, and particles below 1,000 nm diameter are usually more desirable for better insulin absorption through the intestinal milieu.[22] Particle size of insulin loaded CS/ALG and CS-g-PAMAM/ALG core-shell nanoparticle was determined by dynamic light scattering as presented in Fig. 2a. It is noticed that the particle size of CS-g-PAMAM/ALG core-shell nanoparticle at different weight ratios varies within the range of 84-194 nm. Whereas, the particle size range of unmodified CS/ALG insulin nanoparticles at similar weight ratio are comparatively larger and vary between 98-216 nm.[7] This can be attributed to the availability of more number of positive charges on the surface of CS-g-PAMAM (due to grafting of PAMAM) compared to the native CS, thereby resulted in more tight entrapment of excess insulin to form smaller nanoparticles. Again, a slight increase in particle size is observed with further augmentation in polymer concentration; this has happened due to the generation of strong repulsion force between excess positive charges on the surface of polymeric molecules after complete electrostatic interaction with the negatively charged insulin. Similar results are also found in our earlier reports.[8,17] In previous studies, insulin loaded CS/ALG nanoparticles (98-216 nm)[7] and dendronized CS/insulin self assembled nanocomplexes (80-175 nm) are used for oral insulin delivery[17]; other polymeric systems with particle size of 200 nm are also reported for insulin delivery.[38] In the present work, the particle size of the core-shell nanoparticles is much smaller as compared to the earlier investigation.[7] Therefore, the core-shell particles could serve as better oral insulin carrier through the intestinal cells.[39]

The zeta potential values of the insulin loaded CS/ALG and CS-g-PAMAM/ALG core-shell nanoparticles are shown in Fig. 2b and are compared with those of insulin. The zeta value of insulin is -11.64 mV, whereas a sharp increase in zeta potential of insulin loaded CS/ALG and CS-g-PAMAM/ALG core-shell nanoparticles at 0.25:3:1 weight ratio is observed and they are found to be as +.75 mV and +.93 mV, respectively. Again, further increase in zeta potential was noticed with increasing weight ratio of polymers (0.5:3:1, 1:3:1, 2:3:1 and 3:3:1) in the formation of core-shell nanocomplexes as shown in Fig. 2b. The zeta potential of the nanoparticles is positive, where as insulin is negatively charged (-11.64 mv). This may possibly happen due to the presence of excess positive charges in CS and CS-g-PAMAM after the neutralization of entire the negative charges on the insulin molecules (Fig. 2b). Again, CS-g-PAMAM carries comparatively more surface cationic charges than unmodified CS, thus the zeta potential of CS-g-PAMAM/ALG/INS nanoparticles shows more positive zeta value compared to insulin loaded CS/ALG nanocomplexes. So, positive zeta potential of core-shell particles could successfully prolong the interaction time with negatively charged intestinal mucus layer that in turn facilitate sustained release of entrapped insulin by increasing the stability and providing effective protection against self-aggregation.

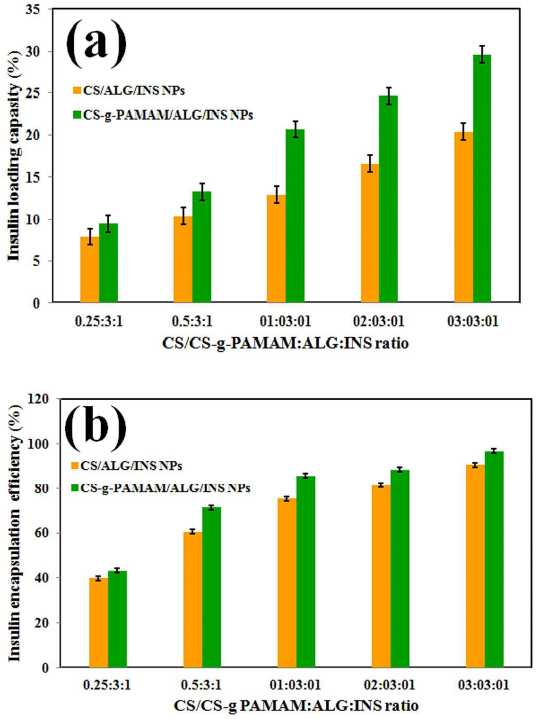

Fig. 4 Comparative study of (a) insulin loading capacity and (b) Percentage of insulin encapsulation of insulin loaded CS/ALG and CS-g-PAMAM/ALG core-shell nanoparticles.

3.3. Scanning electron microscopy (SEM)

The insulin loaded CS/ALG and CS-g-PAMAM/ALG core-shell nanoparticles are morphologically characterized using SEM as shown in Fig. 3. The micrographs show that the nanoparticles (1:3:1 weight ratio) have smooth surface and distinct spherical shape as found in the earlier report.[7] The core-shell structures of the nanoparticles from different composition are also very distinct from the SEM observations. The diameter of the insulin loaded CS-g-PAMAM/ALG nanoparticles is roughly within the size range of 50-78 nm (Fig. 3b), much smaller as compared to unmodified CS/ALG nanoparticles with size between 95-150 nm (Fig. 3a) at the same weight ratio. These results are quite consistent with the DLS measurement. Again, the higher numbers of cationic charges offered by CS-g-PAMAM (due to grafting of PAMAM) are able to tightly condense higher amount of negatively charged insulin and resulted in smaller particles compared to native CS. An Independent scattering of the core-shell nanoparticles under SEM suggests possible stabilization against self-aggregation. Our previous reports also demonstrated similar results.[7] However, the particle size observed in SEM study found to be smaller compared to those obtained from DLS analysis. This may be attributed to the higher hydrodynamic diameter of freshly prepared nanoparticles measured by DLS, whereas SEM images can nullify the swelling effects.

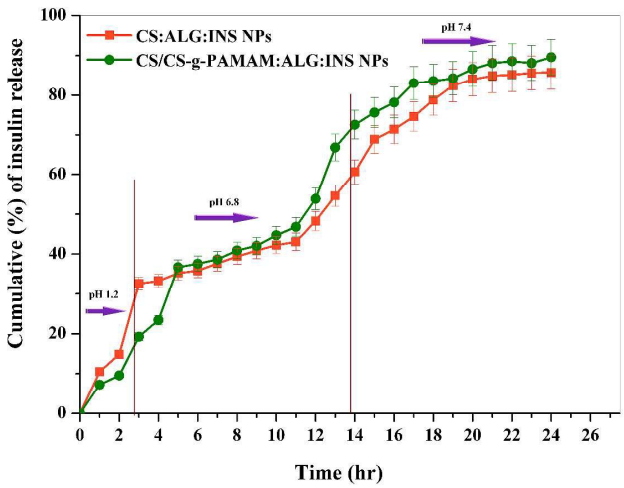

Fig. 5 Cumulative insulin release profile of CS/ALG and CS-g-PAMAM/ALG core-shell nanoparticles at different pH corresponding to GI tract (i.e., pH 1.2, pH 6.8 and pH 7.4).

3.4. Insulin loading and encapsulation efficiency of core-shell nanoparticles

Successful oral insulin delivery by polymeric nanoparticle demands significant insulin encapsulation and loading capacity. Because poor insulin encapsulation efficiency could limit the wide use of polymeric nanoformulations as it would not be able to pursue the desired functions following oral administration. Therefore, percentage of insulin loading capacity and insulin encapsulation of these insulin loaded CS/ALG and CS-g-PAMAM/ALG core-shell nanoparticles with different weight ratios of CS or CS-g-PAMAM:ALG:INS (0.25:3:1, 0.5:3:1, 1:3:1, 2:3:1 and 3:3:1) were investigated, as shown in Fig. 4a and Fig. 4b, respectively. The percentage of insulin loading capacity of CS/ALG nanoparticles at different weight ratios varies between 8-20% and maximum encapsulation efficiency was found to be ~ 90% (weight ratio of 3:3:1); whereas, CS-g-PAMAM/ALG core-shell nanoparticles at same weight ratios provided better insulin loading (10-29%) and showed a maximum insulin encapsulation efficiency of ~ 97%. It is observed from the study that insulin encapsulation efficiency was improved with increasing amount of CS or CS-g-PAMAM used in nanoparticle formation. A fixed amount of ALG was used in all of the compositions of the core-shell nanoparticles to ensure that calcium ALG was maintained in the pre-gel state to enable the proper ionic interactions between ALG, calcium, and cationic polymer CS or CS-g-PAMAM to form nanoparticles. Again, CS-g-PAMAM formulated nanoparticles showed better encapsulation as compared to unmodified CS. This can be explained by the fact that CS-g-PAMAM carries more cationic charges than unmodified CS, leading to a stronger ionic interaction between the negative charges of insulin present in the ALG core and the positive charges of CS-g-PAMAM; this may result in better loading capacity and elevated insulin encapsulation. However,

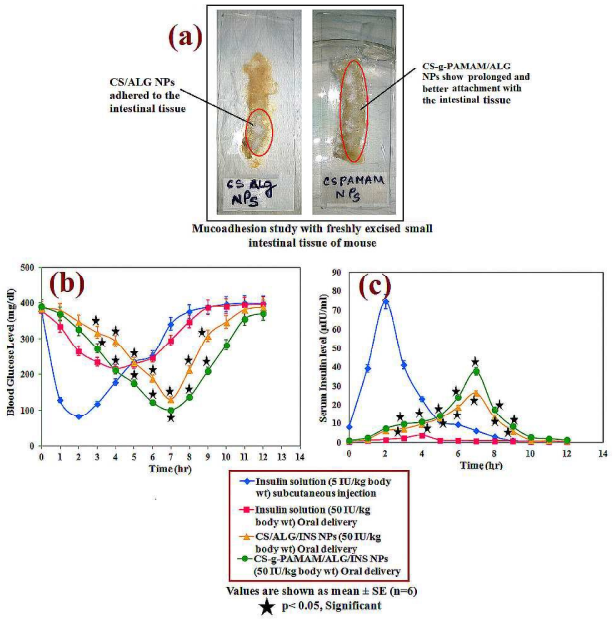

Fig. 6 (a) mucoadhesion study in excised animal tissue, (b) *in vivo* pharmacological response and (c) serum insulin concentration after peroral treatment of CS/ALG and CS-g-PAMAM/ALG core-shell nanoparticles.

nanoparticles with CS or CS-g-PAMAM:ALG:INS weight ratio of 1:3:1 was further used for *in vitro* and *in vivo* studies due to its smaller particle size (from DLS analysis) and significant insulin encapsulation and loading with comparatively less amount of polymers. This composition could be easily internalized through tight junction between intestinal cells for exerting desired functions in diabetics.

3.5. *In vitro* insulin release profile from nanoparticles

The cumulative insulin release profile of both insulin loaded CS/ALG and CS-g-PAMAM/ALG nanoparticles are investigated in pH gradient manner at different pH corresponding to the GI tract, i.e., pH 2.0 (simulated gastric fluid, SGF), pH 6.8, duodenum, and 7.4 (simulated intestinal fluid, SIF) [ileum] at 37 ± 0.5 ºC as illustrated in Fig. 5. Initially, a burst release occurred in case of both the core-shell nanoformulations (CS/ALG and CS-g-PAMAM/ALG) in simulated gastric media (pH 1.2) followed by a slow and modulated release kinetics. The immediate release at pH 1.2 might happen because of weak interaction between insulin and the polyelectrolytes on their surface. As documented, maximum 32.6 % and 27% insulin was released at pH 1.2 after 2 hr in case of CS/ALG and CS-g-PAMAM/ALG nanoparticles, respectively. Then, the nanoparticle formulations were transferred to simulated intestinal fluid (SIF, pH 6.8 and 7.4), where, a sustained and prolonged insulin release was observed eluting 71-85 % and 72-89% of the initial amount from CS/ALG and CS-g-PAMAM/ALG core-shell particles, respectively. Again, more positively charged CS-g-PAMAM shell and tight network of ALG core helps in retaining higher amount of insulin at a lower pH of 1.2 than unmodified CS; it is expected that this might provide effective protection to the encapsulated insulin against the proteolytic degradation in stomach. On the contrary, at pH 6.8 and 7.4, the sustained and prolonged insulin release from core-shell nanoparticles has been achieved due to the increased interaction between alkaline solvent and positively charged CS and CS-g-PAMAM shell, aiding better penetration of the solvent towards the ALG core where insulin is present; solvent could further penetrate inside the ALG core by diffusion process, thereby releasing significant amount of entrapped insulin. The swelling property of ALG at an alkaline media leading to an ionic state may also contribute towards higher insulin release. Therefore, CS-g-PAMAM/ALG core-shell nanoparticles are found to be efficient in protecting the insulin in acidic environment minimizing the insulin loss in the stomach, thereby facilitating successful oral delivery of insulin *in vivo*.

Generally, in several experimental conditions, drug release mechanism from swellable polymeric formulations follows a non-Fickian (anomalous) behaviour The mechanism of drug release from erodible, hydrophilic polymer matrices is a complex process, because several physical factors are involved, such as penetration of water into the polymeric matrix with consequent swelling and solubilisation/erosion of the polymeric formulation and dissolution of the drug from the swollen matrix etc. In such type of release mechanism Ritger-Peppas model is usually fitted.

Therefore, in the present study, to determine the actual mechanism of insulin release in the pH gradient medium from the polymeric core shell nanoparticles, the parameter '*n*' of the Ritger-Peppas equation was computed. The correlation coefficient values in case of CS/ALG and CS-g-PAMAM/ALG nanoparticles were found to be 0.7799 and 0.7969 respectively, (R≥0.99); this clearly indicates that the release data is well fitted to the empirical equation. The "*n*" release exponent is ranged between 0.88-0.89 (0.8898 ± 0.07 in case of CS/ALG nanoparticles and 0.8999 ± 0.04 in case of CS-g-PAMAM/ALG nanoparticles), indicating a non-Fickian (anomalous) transport ($0.45 < n < 0.89$) for both the tested nanoparticles.[32,33] Therefore, the results indicate towards diffusion controlled as well as swelling controlled insulin release kinetics (anomalous transport or non-Fickian diffusion mechanism) from the CS/ALG and CS-g-PAMAM/ALG core-shell nanoparticles.

3.6. Mucoadhesion and *In vivo* pharmacological response of Core-shell particles

The Fig. 6a clearly demonstrates significant mucoadhesion of the core-shell nanoparticles being firmly attached to freshly cut mouse intestinal lumen after continuous washing with buffer (pH 7.4) for 30 min. The mucoadhesive property of the nanoparticles could be attributed to the mucoadhesive

nature[40] and adsorption enhancing properties of CS,[1,22,41,] CS-g-PAMAM and ALG,[24] which might have contributed to such prolonged attachment with the intestinal wall. Furthermore, CS and modified CS could reversibly open the tight junctions of intestinal epithelial cells,[42] allowing progressive internalization of the nanoparticles. Again, strong interaction between the positive charged amino groups of CS-g-PAMAM and the negatively charged sialic-acid groups of mucin could have offered easy penetration resulting in sustained release of encapsulated insulin in the intestine lumen. The effective size of core-shell nanoparticles might enable prolonged hypoglycaemic response via microfold cell (M cell) mediated uptake of insulin loaded core-shell nanoparticles overlaying the intestinal Peyer's patches.[43]

In vivo pharmacological responses of CS/ALG and CS-g-PAMAM/ALG core-shell nanoparticles following peroral treatment in diabetic mice are illustrated in Fig. 6b. Both the core-shell nanoparticles show hypoglycaemic effects when delivered orally, as compared to the control one (subcutaneous injection of insulin 5 IU/kg b.w.). But CS-g-PAMAM/ALG core-shell nanoparticles exhibited more pronounced effects in the lowering of blood glucose level compared to CS/ALG core-shell nanoparticles. After subcutaneous injection, the blood glucose level starts lowering significantly within 30-45 min and reaches 82 mg/dL at 2nd hr of post administration. But, the hypoglycemic effect sustains for only 2 hr further and subsequently returns to its basal level at the 5th hr onwards after administration (Fig. 6b). On the contrary, oral administration of CS/ALG and CS-g-PAMAM/ALG core-shell nanoparticles (both 50 IUkg^{-1} b.w.) resulted in the significant reduction of glycemia. In case of these core-shell nanoparticles, the reduction in the blood sugar level in diabetic animal initiated 2-3 hr post administration and hypoglycemic episode continued up to 7 to 8 hrs. However, the CS-g-PAMAM/ALG core-shell nanoparticles exhibited better sustained hypoglycemic effects for 8 hrs, reducing the blood glucose level up to 101 mg/dL compared to CS/ALG core-shell nanoparticles. The CS/ALG shell nanoparticles could lower the glucose level up to 131 mg/dL and the effects sustained for another 30-45 mins.

The corresponding serum insulin concentrations at different time interval after oral delivery of core-shell nanoparticles were investigated and plotted as Fig. 6c. It is observed from the graph that the control group (with subcutaneous insulin injection) resulted in a maximum serum insulin concentration at 2 hr post injection, indicating direct and rapid absorption of insulin into the blood stream. But oral administration of insulin loaded CS/ALG and CS-g-PAMAM/ALG core-shell nanoparticles at a dose of 50 IU kg^{-1} b.w showed a maximum serum insulin concentration at the 7th hr of administration, suggesting successful internalization of the insulin loaded nanoformulations through intestinal epithelial cells with their effective ability to stabilize and protect encapsulated insulin from the enzymatic degradation in the GI tract. Again, CS-g-PAMAM/ALG nanoparticles exhibited more serum insulin concentration as compared to native CS/ALG particles and the effect sustained for another 45-60 mins. In contrast, a negligible amount of serum insulin (bovine insulin) was detected after oral administration of free insulin solution (not encapsulated), because of the absorption of smaller fraction of insulin by the insulin specific receptors located in the intestinal enterocytes. The overall variability in the results was quite similar and comparable to the previously reported investigations.[7,44,45,46]

From the AUC $_{(0–10h)}$ data of the orally delivered insulin loaded CS-g-PAMAM/ALG core-shell nanoparticles treated animal groups, the relative insulin bioavailability is found to be ~11.78%, whereas ~8.84% relative bioavailability of insulin was obtained with CS/ALG nanoparticles, which is significantly higher as comparison to free oral insulin treated group. It is noticed that CS-g-PAMAM/ALG core-shell nanoparticles produced significantly higher bioavailability, indicating effective absorption of insulin in an active form. Generally, the oral insulin bioavailability trials have been reported to be low. For instance, only <2.5% insulin bioavailability has been reported with pH-responsive poly(methacrylicg-ethylene glycol) hydrogel microparticles;[44] ~4% bioavailability has been shown with chitosan nanoparticles after peroral delivery;[45] 7% insulin bioavailability was found using Alginate/Chitosan nanoparticles;[28] ~4.43% insulin bioavailability was observed in our previous study with *N*-succinyl chitosan grafted polyacrylamide hydrogels[13] and ~9.19% oral insulin relative bioavailability was found in our earlier report with dendronized chitosan insulin self-assembled nanoparticles.[17] Recently, Jain et al.[47] have reported two fold increase in oral insulin bioavailability with folate-(FA) coupled polyethylene glycol (PEG)ylated polylactide-co-glycolide (PLGA) nanoparticles in diabetic rat models. Malathi et al, in 2015 showed effective reduction in blood glucose level by oral administration of insulin loaded d-α-tocopherol poly(ethylene glycol) 1000 succinate (TPGS)-emulsified poly(ethylene glycol) (PEG)-capped poly(lactic-co-glycolic acid) (PLGA) nanoparticles.[48] Again, Pechenkin and his group have shown ~10% oral bioavailability of insulin in rat model using chitosan-dextran sulfate microparticles.[49] In the present study, the bioavailability is ~11.78%, which is considerably higher in comparison to the previously reported study with CS/ALG core-shell nanoparticles (~8.11% oral bioavailability).[7] Both CS-g-PAMAM and ALG being mucoadhesive in nature may have contributed to prolonged attachment with the intestinal milieu. Furthermore, CS-g-PAMAM can alter tight junction reversibly better than native CS, without compromising the epithelial cell architecture and viability; this in turn allows maximum insulin interaction and permeation in to the blood stream that finally overcoming the intestinal barriers.[7,28] So, it is observed that CS-g-PAMAM/ALG nanoparticles could provide well protection to insulin from enzymatic degradation, by sheltering insulin within the core-shell structure of the

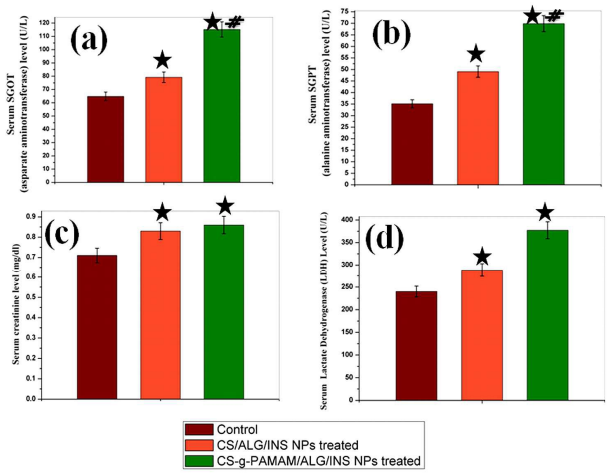

Fig. 7 Acute hepato-toxicity study of CS/ALG and CS-g-PAMAM/ALG core-shell nanoparticle-treated animals, (a) serum SGOT, (b) serum SGPT, (c) serum creatinine, (d) serum LDH.

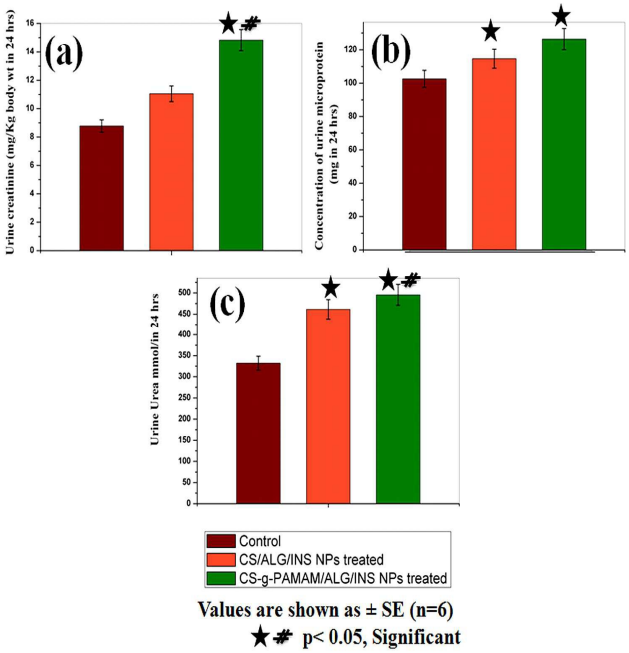

Fig. 8 Acute nephro-toxicity study of CS/ALG and CS-g-PAMAM/ALG core-shell nanoparticle-treated animals, (a) urine creatinine, (b) urine microprotein and (c) urine urea.

nanoparticles. As the GI tract enzymes (pepsin and trypsin) are positively charged species, they cannot bind to the positively charged core-shell nanoparticles. On the other hand, an intimate contact of the nanoparticles with the intestinal wall is established. This allows significant insulin absorption, although some amount of released insulin is probably damaged by the classical degradation phenomena during its GI tract transit. However, the zwitterionic chitosan/PAMAM complex has been documented as a potential carrier of drug to solid tumors,[50] but in the present study, core-shell nanoparticles of PAMAM grafted chitosan/alginate for oral insulin delivery demonstrated excellent hypoglycemic effects *in vivo*.

3.7. Evaluation of in vivo toxicity after oral administration of core-shell nanoparticles

3.7.1. Minimum lethal dose (MLD)

No mortality was observed up to the dose of 300 mg kg^{-1} b.w of core-shell nanoparticles, suggesting a safe polymeric carrier for oral insulin.

3.7.2. Hepato-toxicity analysis

As liver specific enzyme ASAT (asparate aminotransferase) and ALAT (alanine aminotransferase) are significantly elevated in hepatobilliary diseases, and also they have a direct correlation with liver parenchymal damage, ALAT and ASAT level were measured in perorally delivered CS/ALG and CS-g-PAMAM/ALG nanoparticle treated animals and were compared to the control group. It is observed from the Fig. 7a that the ASAT value of control animal is 64.81 U/L and for CS/ALG nanoparticle (300 mg kg^{-1} b.w) treated animal, it is 79.2 U/L, whereas it is 115.23 U/L in CS-g-PAMAM/ALG nanoparticle (300 mg kg^{-1} b.w) treated group. Significant change after oral treatment of nanoparticles is observed as compared to the control one but all the SGOT values are within the reference range of 55-251 U/L of the mouse. Further, ASAT value of control animal is 35.11 U/L, and for CS/ALG and CS-g-PAMAM/ALG nanoparticle (300 mg kg^{-1} b.w) treated animal, it is 49.06 U/L and 69.88 U/L, respectively (Fig. 7b). Although, significant changes in SGPT value of nanoparticle treated animal are found in comparison to the control group, but the values come within the reference range of 28-184 U/L in mouse.[13] Similarly, it can be interpreted from the obtained results that neither liver is damaged nor the liver function is disrupted by peroral treatment of core-shell nanoparticles. The serum creatinine level is 0.71 mg/dL for the control animal, 0.83 mg/dL for the CS/ALG nanoparticles treated animals and 0.86 mg/dL for the CS-g-PAMAM/ALG nanoparticles treated animals (Fig. 7c), where the normal reference range is 0.7-1.1 mg/dL. Again, it is noticed from Fig. 7d that the serum LDH value of the control animal group is 240.1 U/L and it is 288.6 U/L and 377. 42 U/L in CS/ALG and CS-g-PAMAM/ALG nanoparticles (300 mg kg^{-1} b.w) treated mice. Although, significant change is found as compared to the control one, still the LDH values are within the normal reference range of 230-460 U/L. So, from these serum parameters, it can be interpreted that no liver damage, no toxicological and functional disorder have occurred in the

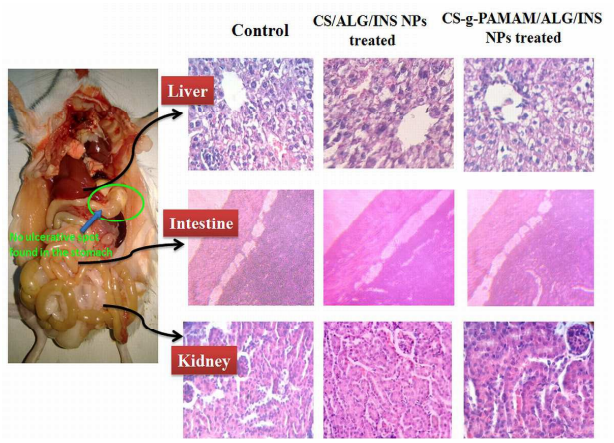

Fig. 9 Internal organs of a treated animal and sections of liver, intestine and kidney (H&E staining, magnification 40x) of control and treated (peroral insulin loaded CS/ALG and CS-g-PAMAM/ALG core-shell nanoparticles) mice.

animals by the peroral treatment of CS-g-PAMAM/ALG core-shell nanoparticles.

3.7.3. Assessment of nephro-toxicity

To assess the nephro-toxicity, serum creatinine is most commonly measured. A sharp rise in the serum creatinine level indicates the marked damage to the functioning nephrons. The serum creatinine concentration of core-shell nanoparticle treated mice fall within normal reference range (0.7-1.1 mg/dL) indicating no acute oral toxicity. Urine creatinine is an indicator of the urinary tract obstruction, kidney failure, dehydration, severe kidney disease, shock, renal outflow obstruction and acute tubular necrosis. Therefore, the concentration of urine creatinine is measured and presented in the Fig 8a. The creatinine value in control mice is 8.78 mg kg^{-1} b.w., it is 11.05 and 14.83 mg kg^{-1} b.w. in CS/ALG and CS-g-PAMAM/ALG nanoparticle (300 mg kg^{-1} b.w.) treated mice, respectively. The values are within the reference range (8.4-24.6 mg/kg b.w), indicating no nephro-toxicity. Proteins (albumin and globulin fractions) are known to involve in the maintenance of normal distribution of water between blood and the tissues. Proteinuria may result from increased glomerular permeability or defective tubular reabsorption. Therefore, urine microprotein was assayed after peroral treatment of CS/ALG and CS-g-PAMAM core-shell nanoparticle for evaluating the renal disease or glomerular damage. The concentration of urine microprotein in control animal is 102.55 mg/24 hr, and for CS/ALG and CS-g-PAMAM core-shell nanoparticles (300 mg kg^{-1} b.w) treated animals, it is observed to be 114.64 mg/24 hr and 126.41 mg/24 hr (Fig. 8b). A significant change is found as compared to the control one, but values fall within normal microprotein reference range

Table 2 Qualitative analysis of different biochemical parameters of urine in CS/ALG and CS-g-PAMAM/ALG nanoparticle-treated animals.

Parameters	Control animal (treated with 0.9% NaCl)	Peroral treatment with CS/ALG/INS nanoparticles (300mg/ Kg b.w)	Peroral treatment with CS-g-PAMAM/ALG/INS nanoparticles (300mg/ Kg b.w)
Urobilinogen	0.2	0.2	0.2
Protein	Negligible	Trace	trace
pH	7.5	7.5	8.0
Blood	Moderate (Non-Haemolysed)	Moderate (Haemolysed)	Trace (Haemolysed)
Specific gravity	1.005	1.020	1.015
Ketone	Negligible	Negligible	Negligible
Bilirubin	Negligible	+	Negligible
Glucose	Negligible	Negligible	Negligible

(28-140 mg/24 hr), ensuring no renal dysfunction. Moreover, concentration of urea in urine is also measured and shown in Fig. 8c. The urea concentration is 495.64 mmol in 24 hr for the CS-g-PAMAM/ALG core-shell nanoparticle (300 mg kg^{-1} b.w.) treated animals and 461.33 mmol in 24 hr for the CS/ALG core-shell nanoparticles treated mice (300 mg kg^{-1} b.w.). A significant change is observed as compared to the control animal group (332.21 mmol in 24 hr), although these values are within the reference range of 333-583 mmol/24hr. So, all these studies suggest that the CS-g-PAMAM/ALG core-shell nanoparticle could be a safe polymer for oral insulin delivery.

Again, pathohistological study revealed no damage to liver, kidney and intestinal tissues of treated mice, after H&E (hematoxylin and eosin) staining (Fig. 9). The results are quite consistent with our previous report.[51] The stomach was also examined. No ulcerative spot was noticed in the stomach after nanoparticle treatment as shown in Fig 9. This suggests that the stomach is not affected by the polymeric core-shell nanoparticles. Overall, in pathohistology, the appearance of

CS/ALG and CS-g-PAMAM core-shell nanoparticle treated liver sections are almost similar to that of the control tissue; central vein with radiating hepatic cells are observed, illustrating no apparent hepato-toxicity after nanoparticle administration. Further, the section of the kidney of CS/ALG, CS-g-PAMAM core-shell nanoparticle treated animal and the control one show the presence of the renal corpuscle surrounded by Bowman's capsule; kidney tubules are lined by simple cuboidal epithelium. A urinary space (appears as a clear space) was also visible on these histological slides. The glomerulus, a tuft of capillaries also appears as a large cellular mass. These observations imply that no renal toxicity after oral treatment of the polymeric core-shell nanoparticles in animal model is observed.

Moreover, the qualitative analysis of different biochemical parameters (Table 2) of urine, showed no significant alteration after treatment with CS/ALG and CS-g-PAMAM core-shell nanoparticle. So, it can be interpreted from the acute toxicity study that the core-shell nanoparticles of CS-g-PAMAM/ALG could be a safe polymeric carrier for successful oral insulin delivery.

4. Conclusions

The low toxic, water soluble chitosan derivative, CS-g-PAMAM is successfully prepared for oral insulin delivery. The present study concludes successful preparation and characterization of insulin loaded CS-g-PAMAM/ALG core-shell nanoparticles in *in vitro* and *in vivo* systems. The almost spherical, core-shell structured nanoparticles showed ~29% insulin loading and ~97% insulin encapsulation efficiency and a pH responsive insulin release. The core-shell nanoparticles are able to establish a prolonged hypoglycemic effect compared to those obtained from free oral insulin and native CS/ALG core-shell nanoparticles, revealing significant enhanced relative oral insulin bioavailability (~11.78%) compared to unmodified CS/ALG core-shell nanoparticles (~8.84%). Since, no systemic toxicity is observed in acute experimental trials, one can assure that the CS-g-PAMAM/ALG core-shell nanoparticles could be a promising polymeric vehicle in oral insulin or other therapeutic drugs due to its efficient and safe mode of administration.

Acknowledgements

We are highly grateful to Department of Science and Technology, Government of West Bengal for their financial support for this work and the project entitled 'Synthesis of derivatives of chitosan and their IPNs for oral insulin delivery'; Sanction No.428 (Sanc.)/ST/P/S & T/2G-7/2011).

Notes and references

[a] *Department of Polymer Science and Technology, 92, A.P.C. Road, Kolkata-700009, University of Calcutta, India. Fax: 91-2352-5106; Tel: 91-2352-5106; E-mail:* ppk923@yahoo.com

1 P. Mukhopadhyay, R. Mishra, D. Rana, and P. P. Kundu, *Prog. Polym. Sci.,* 2012, **37**, 1457.
2 A. Chaudhury and S. Das, *AAPS Pharm.Sci.Tech.,* 2011, **12**, 10.
3 A. k. Prusty and S. K. Sahu, *ISRN Nanotechnology, 2013,* **2013***, 1.*
4 S. Olya, M. Khorvash, H. R. Rahmani, S. Esmaeilkhanian, B. Olya, H. Sadri, *Czech J. Anim. Sci.,* 2014, **59**, 251.
5 Z. M. Wu, L. Ling, L. Y. Zhou, X. D. Guo, W. Jiang, Yu. Qian, K. Q. Luo, and L. J. Zhang, *Nanoscale. Res. Lett.,* 2012, **7**, 299.
6 J. R. Azevedo, R. H. Sizilio, M. B. Brito, A. M. B. Costa, M. R. Serafini, A. A. S. Araújo, M. R. V. Santos, A. A. M. Lira, and R. S. Nunes, *J. Therm. Anal. Calorim*., 2011, **106**, 685.
7 P. Mukhopadhyay, S. Chakraborty, S. Bhattacharya, R. Mishra and P. P. Kundu, *Int. J. Biol. Macromol*., 2015, **72**, 640.
8 P. Mukhopadhyay, K. Sarkar, M. Chakraborty, S. Bhattacharya, R. Mishra, and P. P. Kundu, *Mater. Sci. Eng., C,* 2013, **33**, 376.
9 K. Nagpal, S. K. Singh, D. N. Mishra, *Chem. Pharm. Bull.*, 2010, **58**, 1423.
10 H.L. Luessen, B.J. de Leeuw, M.W. Langemeÿer, A.B. de Boer, J.C. Verhoef, H.E. Junginger, *Pharm. Res*, 1996, **13**, 1668.
11 S. Aiba, *Int. J. Biol. Macromol*., 1992, **14**, 225.
12 S. Hiran, H. Seino, Y. Akiyama, I. Nonaka, *Polym. Eng. Sci.*, 1988, **59**, 897.
13 P. Mukhopadhyay, K. Sarkar, S. Bhattacharya, A. Bhattacharyya, R. Mishra and P. P. Kundu, *Carbohydr. Polym.*, 2014, **112**, 627.
14 E. A. Stepnova, V. E. Tikhonov, T. A. Babushkina, T. P. Klimova, E. V. Vorontsov, V. G. Babak, S. A. Lopatin, and I. A.Yamskov, *Eur. Polym. J.*, 2007, **43**, 2414.
15 R. A. A. Muzzarelli, and F. Tanfani, *Carbohydr. Polym*., 1985, **5**, 297.
16 H. Sashiwa, N. Kawasaki, A. Nakayama, E. Muraki, N. Yamamoto, and S.I. Aiba, *Biomacromolecules*, 2002, **3**, 1126.
17 P. Mukhopadhyay, K. Sarkar, S. Bhattacharya, R. Mishra and P. P. Kundu, *RSC Adv*., 2014, **4**, 43890.
18 N. M. Alves, J. F. Mano, *Int. J. Biol. Macromol*., 2008, **43**, 401.
19 R. Esfand, and D. A. Tomalia, *Drug Discovery Today*, 2001, **6**, 427.
20 S. Sadekar, H. Ghandehari, *Adv. Drug. Deliv. Rev.,* 2012, **64**, 571.
21 Svenson, and D. A. Tomalia, *Adv. Drug Deliv. Rev*., 2005, **57**, 2106.
22 R. Duncan, and L. Izzo, *Adv. Drug Deliv. Rev.,*2005, **57**, 2215.
23 J. Dusseault, F. A. Leblond, R. Robitaille, G. Jourdan, J. Tessier, M. Ménard. N. Henley, J.P. Hallé, *Biomaterials*, 2005, **26**, 1515.
24 M. George, T. E. Abraham, *J. Control. Release.*, 2006, **114**, 1.
25 E. Esposito, R. Cortesi, C. Nastruzzi, *Biomaterials*, 1996, **17**, 2009.
26 P. R. Hari, T. Chandy, C. P. Sharma, *J Microencapsul.*, 1996, **13**, 319.
27 B. Sarmento, A. J. Ribeiro, F. Veiga, D. C. Ferreira, R. J. Neufeld, *J Nanosci Nanotechnol*., 2007, **7**, 2833.
28 B. Sarmento, A. Ribeiro, F. Veiga, P. Sampaio, R. Neufeld, D. Ferreira, *Pharm. Res*., 2007, **24**, 2198.
29 D. A. Tomalia, H. Baker, J. Dewald, M. Hall, G. Kallos, S. Martin, J. Roek, J. Ryder, P. Smith, *Polym. J*., 1985, **17**, 117.
30 H. Sashiwa, Y. Shigemasa, and R. Roy, *Carbohydr. Polym.,* 2002, 47, 201.
31 M. Rajaonarivony, C. Vauthier, G. Couarraze, F. Puisieux, P. Couvreur, *J. Pharm. Sci*., 1993, **82**, 912.
32 P. L. Ritger and N. A. Peppas, *J. Control Release*, 1987, **5**, 37.

33 X. Zhang, Z. Wu, X. Gao, S. Shu, H. Zhang and Z. Wang, *Carbohydr. Polym.*, 2009, **2**, 394.
34 S. Sajeesh and C. P. Sharma, *Int. J. Pharm.*, 2006, **325**, 147.
35 F. Cui, F. Qian, Z. Zhao, L. Yin, C. Tang, C. Yin, *Biomacromolecules.*, 2009, **10**, 1253
36 P. Mukhopadhyay, K. Sarkar, S. Soam, and P. P. Kundu, *J. Appl. Polym. Sci.,* 2013, **129**, 835.
37 S. J. Mahmood, A. Siddique, *J. Saudi Chem. Soc.*, 2010, **14**, 117.
38 F. Cui, K. Shi, L. Zhang, A. Tao, Y. Kawashima, *J. Control. Release*, 2006, **114**, 242.
39 A. Fasano, *Trends Biotechnol*. 1998, **16**, 152.
40 C.-M. Lehr, J. A. Bouwstra, E. H. Schacht, and H. E. Junginger, *Int. J. Pharm.,* 1992, **78**, 43.
41 L. Illum, *Pharm. Res.,* 1998, **15**, 1326.
42 M. Thanou, J. C. Verhoef, and H. E. Junginger., *Adv. Drug Deliv.* Rev., 2001, **50**, 91.
43 C. Prego, D. Torres, and M. J. Alonso., *Opin. Drug Deliv.,* 2005, **2**, 843.
44 A. M. Lowman, M. Morishita, M. Kajita, T. Nagai, N. A. Peppas, *J. Pharm. Sci.*, 1999, **88**, 933.
45 Z. Ma, T. M. Lim, L. Y. Lim, *Int J Pharm., 2005,* **293**, 271.
46 Y. Pan, Y. J. Li, H. Y. Zhao, J. M. Zheng, H. Xu, G. Wei, J. S. Hao, F. D. Cui, *Int J Pharm*., 2002, **249**, 139.
47 S. Jain, V. V. Rathi, A. K. Jain, M. Das, and C. Godugu, *Nanomedicine (Lond).,* 2012, **7**, 1311.
48 S. Malathi, P. Nandhakumar, V. Pandiyan, T. J. Webster, S. Balasubramanian, *Int. J. Nanomedicine.,* 2015, **10,** 2207.
49 M. A. Pechenkin, N. G. Balabushevich, I. N. Zorov, L. K. Staroseltseva, E. V. Mikhalchik, V. A. Izumrudov and N. I. Larionova, *J. Bioequiv. Availab.,* 2011, **3**, 244.
50 K. C. Liu, and Y. Yeo, *Mol. Pharm.*, 2013, **10**, 1695.
51 P. Mukhopadhyay, S. Bhattacharya, A. Nandy, A. Bhattacharyya, R. Mishra and P. P. Kundu, *Toxicol. Res.*, 2015, **4**, 281.